Numerical Synthesis of Six-Bar Linkages for Mechanical Computation

Mark M. Plecnik
Robotics and Automation Laboratory,
University of California,
Irvine, CA 92697
e-mail: mplecnik@uci.edu

J. Michael McCarthy
Robotics and Automation Laboratory,
University of California,
Irvine, CA 92697
e-mail: jmmccart@uci.edu

This paper presents a design procedure for six-bar linkages that use eight accuracy points to approximate a specified input–output function. In the kinematic synthesis of linkages, this is known as the synthesis of a function generator to perform mechanical computation. Our formulation uses isotropic coordinates to define the loop equations of the Watt II, Stephenson II, and Stephenson III six-bar linkages. The result is 22 polynomial equations in 22 unknowns that are solved using the polynomial homotopy software BERTINI. *The bilinear structure of the system yields a polynomial degree of 705,432. Our first run of* BERTINI *generated 92,736 nonsingular solutions, which were used as the basis of a parameter homotopy solution. The algorithm was tested on the design of the Watt II logarithmic function generator patented by Svoboda in 1944. Our algorithm yielded his linkage and 64 others in 129 min of parallel computation on a Mac Pro with 12 × 2.93 GHz processors. Three additional examples are provided as well.*
[DOI: 10.1115/1.4027443]

1 Introduction

This paper presents a methodology for the design of mechanical computers that approximate a function specified by eight angular pairs of accuracy points. This is known as the kinematic synthesis of a function generator, see Refs. [1–4]. In 1944, Svoboda [5,6] used a nomograph formulation to design a six-bar linkage that generates a logarithmic function, which he called a "double three-bar" because it is a Watt II type six-bar that can be viewed as two connected four-bar linkages. More recently, Hwang and Chen [7] presented a methodology for the synthesis of six-bar function generators of the Stephenson II type.

This work uses isotropic coordinates to formulate the loop equations of three types of six-bar linkages that are useful for function generation: the Watt II, Stephenson II, and Stephenson III types, see Fig. 1. For each linkage type, we specify eight pairs of input–output joint angles, (ϕ_j, ψ_j), $j = 1 \ldots 8$, called accuracy points that satisfy a specified input–output function. Two constraint equations and one normalization condition are obtained from each of eight accuracy points which leads to a system of 24 nonlinear equations in 24 unknowns. This system can be simplified to obtain 22 bilinear equations in 22 unknowns, which has a maximum of 705,432 solutions.

The polynomial homotopy continuation software BERTINI was used to solve the synthesis equations to yield 92,736 nonsingular solutions in 107 min on a Mac Pro with 12×2.93 GHz processors. This solution was then used in a parameter homotopy to design linkages for three different examples of function specification.

2 Literature Review

A mechanical computer is a linkage system that calculates an output for a given input, also called a function generator. Svoboda [5] designed function generators by fitting the input–output functions of a given set of linkages to the desired function. He patented a Watt II type six-bar linkage that computed a logarithmic function [6]. Freudenstein [8] introduced a new approach that used the loop equations of a four-bar linkage to fit a given set of accuracy points to obtain a four-bar function generator.

McLarnan in 1963 [9] formulated the loop equations for three types of six-bar linkages, the Watt II, Stephenson II and III types, to design function generators. He obtained algorithms for six, seven, eight, and nine accuracy points for the Watt II six-bar linkage, which were executed on an IBM 704 computer. He obtained two Watt II linkages that achieved seven accuracy points, and noted the problem of the separation of accuracy points on different linkage branches, now known as a branch defect. Three decades later, Dhingra et al. [10] formulated the synthesis equations for Watt II, Stephenson II and III function generators and used a numerical homotopy algorithm to solve these equations. They report 1.5 s to track each of 71,680 homotopy paths for eight accuracy points on an 486 PC. This is approximately 30 h to complete one synthesis calculation, and does not include the analysis of each design to verify that its accuracy points are on the same branch.

Recently, Hwang and Chen [7] formulated the design of Stephenson II six-bar function generators using optimization techniques to find defect-free linkages. Sancibrian [11] takes a similar approach using the generalized reduced gradient to find the linkage parameters that minimize the difference between the input–output function of the linkage and the desired function.

In this paper, we formulate complex versions of the loop equations for the Watt II, Stephenson II and III six-bar linkages and use numerical homotopy to solve the equations, see Refs. [12–14]. Our focus is fitting a function generator to eight accuracy points, which yields 22 synthesis equations in 22 unknowns. In order to find Watt II, and Stephenson II and III six-bar function generators that have the eight accuracy points on a single branch, we also analyze each of the resulting designs to verify its performance.

3 Complex Vectors and Isotropic Coordinates

Erdman et al. [15] formulate planar kinematics using complex numbers to represent the coordinates of points in the plane. In this formulation, the coordinates $P = (P_x, P_y)$ of a point are formulated as the complex number

$$P = P_x + iP_y \tag{1}$$

The component-wise sum of a complex number is the same as for coordinate vectors, and the product of complex numbers performs rotation and scaling operations. In particular, the exponential $\exp(i\theta)$ is a rotation operator on complex vectors that yield

Contributed by the Mechanisms and Robotics Committee of ASME for publication in the JOURNAL OF MECHANISMS AND ROBOTICS. Manuscript received July 31, 2013; final manuscript received April 11, 2014; published online June 17, 2014. Assoc. Editor: Jorge Angeles.

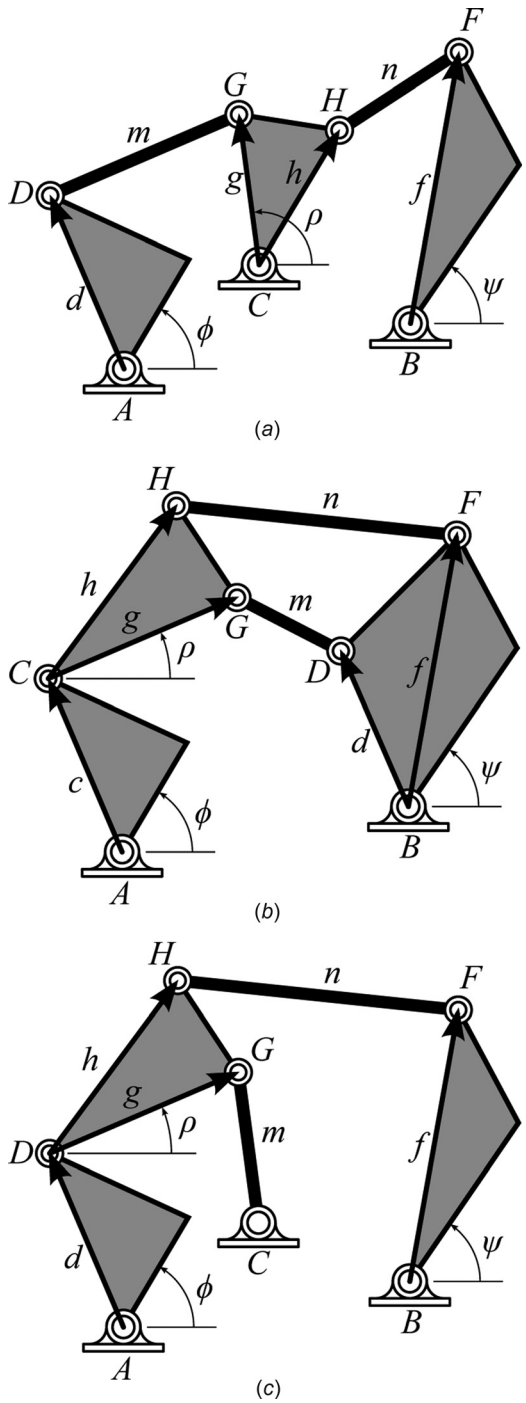

Fig. 1 The three types of Watt and Stephenson six-bar linkages that are useful for mechanical computation at fixed pivots. The angle ϕ at the fixed pivot *A* is the input value and the angle ψ at the fixed pivot *B* is the output value of the function.

the same result as a 2×2 rotation matrix operating on vectors, that is

$$\begin{aligned} P &= e^{i\theta}p, \\ P_x + iP_y &= (\cos\theta + i\sin\theta)(p_x + ip_y), \\ P_x + iP_y &= (\cos\theta p_x - \sin\theta p_y) + i(\sin\theta p_x + \cos\theta p_y) \end{aligned} \tag{2}$$

Wampler [13] shows that it is convenient to consider the complex number P and its conjugate $\bar{P}$ as components of "isotropic coordinates" $(P,\bar{P})$ because the original components are obtained from the linear transformations

$$P_x = \frac{1}{2}(P+\bar{P}), \quad P_y = \frac{1}{2i}(P-\bar{P}) \tag{3}$$

For our purposes, the reference to isotropic coordinates means that both the complex and complex conjugate loop equations are used in the formulation of the synthesis equations.

4 Synthesis Equations

The formulation of the synthesis equations for Watt II, Stephenson II and III function generators is closely parallel to each other. Note that synthesis of the Watt I and Stephenson I mechanisms was not studied because coordination between their ground pivots results in four-bar synthesis. Function generation between moving pivots was not studied in this paper.

In this section, the loop equations are formulated for each topology, a normalization condition is appended for each accuracy point, then each system of equations is put into the polynomial form shown in Eq. (35). Putting all three topologies into this form allows us to compute solutions to a single general polynomial system that can be used to construct straight-line homotopies for all three topologies that are computationally less expensive [16]. The solutions to these systems using the BERTINI software are described in Sec. 5.

4.1 Watt II Synthesis Equations. The synthesis task for a Watt II function generator (Fig. 1(*a*)) is to coordinate the orientation of links *AD* and *BF* such that they move through the angle pairs (ϕ_j,ψ_j), $j=1,\ldots,8$. Note that the input–output functions between link *CGH* and links *AD* or *BF* are not of interest because these are four-bar function generators.

Three sets of complex numbers are introduced to represent the rotations of links *AD*, *CGH*, and *BF* measured relative to the ground frame

$$\begin{aligned} (Q_j,\bar{Q}_j) &= (e^{i\phi_j}, e^{-i\phi_j}), \\ (R_j,\bar{R}_j) &= (e^{i\rho_j}, e^{-i\rho_j}), \\ (S_j,\bar{S}_j) &= (e^{i\psi_j}, e^{-i\psi_j}), \quad j=1,\ldots,8 \end{aligned} \tag{4}$$

The complex vectors $(Q_j,\bar{Q}_j)$ and $(S_j,\bar{S}_j)$ are known from the task specification, while $(R_j,\bar{R}_j)$ are to be determined in the synthesis process.

The loop equations of the Watt II linkage are formulated to define the two floating links *DG* and *FH*, as

$$\begin{aligned} \mathcal{L}_1\text{:}\quad & G - D = A + Q_j d - C - R_j g, \\ \mathcal{L}_2\text{:}\quad & H - F = B + S_j f - C - R_j h, \quad j=1,\ldots,8 \end{aligned} \tag{5}$$

The constraints that the lengths $m=|G-D|$ and $n=|H-F|$ be constant for the movement of the six-bar linkage yield the equations

$$\begin{aligned} \mathcal{C}_1\text{:}\quad & m^2 = (A + Q_j d - C - R_j g)(\bar{A} + \bar{Q}_j\bar{d} - \bar{C} - \bar{R}_j g), \\ \mathcal{C}_2\text{:}\quad & n^2 = (B + S_j f - C - R_j h)(\bar{B} + \bar{S}_j\bar{f} - \bar{C} - \bar{R}_j\bar{h}), \\ & j=1,\ldots,8 \end{aligned} \tag{6}$$

Note that in the equations above, $g=\bar{g}$ as the angle of ρ measures directly to this complex vector. The 16 constraint equations (6) together with the eight equations defining the pairs $(R_j,\bar{R}_j)$ as unit vectors

$$R_j\bar{R}_j = 1, \quad j=1,\ldots,8 \tag{7}$$

yield 24 synthesis equations. The unknowns of these equations are the 16 values of $(R_j,\bar{R}_j)$ and the eight unknowns $(C,\bar{C},d,\bar{d},f,\bar{f},m,n)$. The designer is free to specify the fixed

pivots A and B and the dimensions g and $(h,\bar{h})$ of the link CGH. Unknowns m and n are eliminated by subtracting the first equations of $\mathcal{C}_1$ and $\mathcal{C}_2$ from the rest of the equations in each set, respectively. Next, the unknowns are placed in seven sets of vectors

$$\begin{aligned}\mathbf{v}_j &= (C,d,R_j,R_1,1), \quad j=2,\ldots,8,\\ \mathbf{w}_j &= (C,f,R_j,R_1,1), \quad j=2,\ldots,8\end{aligned} \tag{8}$$

Then, the synthesis equations can be written in the form

$$\mathbf{v}_j^T[M_j]\bar{\mathbf{v}}_j = \begin{pmatrix} C \\ d \\ R_j \\ R_1 \\ 1 \end{pmatrix}^T \begin{bmatrix} 0 & M_{1j} & M_{2j} & M_{3j} & M_{6j} \\ \bar{M}_{1j} & 0 & M_{4j} & M_{5j} & M_{7j} \\ \bar{M}_{2j} & \bar{M}_{4j} & 0 & 0 & M_{8j} \\ \bar{M}_{3j} & \bar{M}_{5j} & 0 & 0 & -M_{8j} \\ \bar{M}_{6j} & \bar{M}_{7j} & \bar{M}_{8j} & -\bar{M}_{8j} & 0 \end{bmatrix} \begin{pmatrix} \bar{C} \\ \bar{d} \\ \bar{R}_j \\ \bar{R}_1 \\ 1 \end{pmatrix} = 0$$

$$j=2,\ldots,8 \tag{9}$$

where

$$\begin{aligned} &M_{1j} = -\bar{Q}_j + \bar{Q}_1, \quad M_{2j} = g, \quad M_{3j} = -g,\\ &M_{4j} = -Q_j g, \quad M_{5j} = Q_1 g, \quad M_{6j} = 0,\\ &M_{7j} = (Q_j - Q_1)\bar{A}, \quad M_{8j} = -\bar{A}g \end{aligned} \tag{10}$$

and

$$\mathbf{w}_j^T[N_j]\bar{\mathbf{w}}_j = \begin{pmatrix} C \\ f \\ R_j \\ R_1 \\ 1 \end{pmatrix}^T \begin{bmatrix} 0 & N_{1j} & N_{2j} & N_{3j} & N_{6j} \\ \bar{N}_{1j} & 0 & N_{4j} & N_{5j} & N_{7j} \\ \bar{N}_{2j} & \bar{N}_{4j} & 0 & 0 & N_{8j} \\ \bar{N}_{3j} & \bar{N}_{5j} & 0 & 0 & -N_{8j} \\ \bar{N}_{6j} & \bar{N}_{7j} & \bar{N}_{8j} & -\bar{N}_{8j} & 0 \end{bmatrix} \begin{pmatrix} \bar{C} \\ \bar{f} \\ \bar{R}_j \\ \bar{R}_1 \\ 1 \end{pmatrix} = 0$$

$$j=2,\ldots,8 \tag{11}$$

where

$$\begin{aligned} &N_{1j} = -\bar{S}_j + \bar{S}_1, \quad N_{2j} = \bar{h}, \quad N_{3j} = -\bar{h},\\ &N_{4j} = -S_j\bar{h}, \quad N_{5j} = S_1\bar{h}, \quad N_{6j} = 0,\\ &N_{7j} = (S_j - S_1)\bar{B}, \quad N_{8j} = -\bar{B}h \end{aligned} \tag{12}$$

This results in 22 synthesis equations for the Watt II function generator where the first two sets of seven equations are obtained from the constraint equations (9) and (11), and the last set of eight is obtained from the normalization conditions (7). These equations have a bilinear structure

$$\begin{aligned} &\langle C,d,R_j,R_1,1\rangle\langle \bar{C},\bar{d},\bar{R}_j,\bar{R}_1,1\rangle, \quad j=2,\ldots,8,\\ &\langle C,f,R_j,R_1,1\rangle\langle \bar{C},\bar{f},\bar{R}_j,\bar{R}_1,1\rangle, \quad j=2,\ldots,8,\\ &\langle R_j,1\rangle\langle \bar{R}_j,1\rangle, \quad j=1,\ldots,8 \end{aligned} \tag{13}$$

For computation purposes, it is useful to divide the variables into two groups

$$\begin{aligned} &\langle C,d,f,R_1,R_2,R_3,R_4,R_5,R_6,R_7,R_8\rangle,\\ &\langle \bar{C},\bar{d},\bar{f},\bar{R}_1,\bar{R}_2,\bar{R}_3,\bar{R}_4,\bar{R}_5,\bar{R}_6,\bar{R}_7,\bar{R}_8\rangle \end{aligned} \tag{14}$$

The number of solutions to this system and the use of the BERTINI software package in order to solve are discussed in Sec. 5.

4.2 Stephenson II Synthesis Equations. The function generation problem of a Stephenson II linkage (Fig. 1(*b*)) is to move its input link AC and its output link BDF through the angle pairs (ϕ_j,ψ_j), $j=1,\ldots,8$. The orientations of links AC, CGH, and BDF are given by angles ϕ_j, ρ_j, and ψ_j, respectively. The complex vector operators for each of these angles are Q_j, R_j, and S_j, respectively. The exponential definitions of these three operators and their conjugates appear in Eq. (4). The conjugate pairs $(Q_j,\bar{Q}_j)$ and $(S_j,\bar{S}_j)$ are known from the accuracy points and $(R_j,\bar{R}_j)$ is to be determined.

The loop equations are used to express links DG and FH

$$\begin{aligned} &\mathcal{L}_1: \quad G - D = A + Q_j c + R_j g - B - S_j d,\\ &\mathcal{L}_2: \quad H - F = A + Q_j c + R_j h - B - S_j f\\ &\qquad j=1,\ldots,8 \end{aligned} \tag{15}$$

These links are constrained to the constant lengths $m=|G-D|$ and $n=|H-F|$, yielding the equations

$$\begin{aligned} &\mathcal{C}_1: \ m^2 = (A + Q_j c + R_j g - B - S_j d)(\bar{A} + \bar{Q}_j\bar{c} + \bar{R}_j g - \bar{B} - \bar{S}_j\bar{d}),\\ &\mathcal{C}_2: \ n^2 = (A + Q_j c + R_j h - B - S_j f)(\bar{A} + \bar{Q}_j\bar{c} + \bar{R}_j\bar{h} - \bar{B} - \bar{S}_j\bar{f}),\\ &\qquad j=1,\ldots,8 \end{aligned} \tag{16}$$

These 16 constraint equations along with the eight normalization conditions

$$R_j\bar{R}_j = 1, \quad j=1,\ldots,8 \tag{17}$$

yield 24 synthesis equations in the 24 unknowns $(R_j,\bar{R}_j)$ and $(c,\bar{c},d,\bar{d},f,\bar{f},m,n)$. Fixed pivots A and B are specified as well as the dimensions g and $(h,\bar{h})$ of link CGH. Unknowns m and n are eliminated by subtracting the first equations of $\mathcal{C}_1$ and $\mathcal{C}_2$ from the rest of the equations in each set, respectively. Next, the unknowns are placed in seven sets of vectors

$$\begin{aligned}\mathbf{v}_j &= (c,d,R_j,R_1,1), \quad j=2,\ldots,8,\\ \mathbf{w}_j &= (c,f,R_j,R_1,1), \quad j=2,\ldots,8\end{aligned} \tag{18}$$

Then, the synthesis equations can be written in the form

$$\mathbf{v}_j^T[M_j]\bar{\mathbf{v}}_j = \begin{pmatrix} c \\ d \\ R_j \\ R_1 \\ 1 \end{pmatrix}^T \begin{bmatrix} 0 & M_{1j} & M_{2j} & M_{3j} & M_{6j} \\ \bar{M}_{1j} & 0 & M_{4j} & M_{5j} & M_{7j} \\ \bar{M}_{2j} & \bar{M}_{4j} & 0 & 0 & M_{8j} \\ \bar{M}_{3j} & \bar{M}_{5j} & 0 & 0 & -M_{8j} \\ \bar{M}_{6j} & \bar{M}_{7j} & \bar{M}_{8j} & -\bar{M}_{8j} & 0 \end{bmatrix} \begin{pmatrix} \bar{c} \\ \bar{d} \\ \bar{R}_j \\ \bar{R}_1 \\ 1 \end{pmatrix} = 0$$

$$j=2,\ldots,8 \tag{19}$$

where

$$\begin{aligned} &M_{1j} = -Q_j\bar{S}_j + Q_1\bar{S}_1, \quad M_{2j} = Q_j g, \quad M_{3j} = -Q_1 g,\\ &M_{4j} = -S_j g, \quad M_{5j} = S_1 g, \quad M_{6j} = (Q_j - Q_1)(\bar{A} - \bar{B}),\\ &M_{7j} = -(S_j - S_1)(\bar{A} - \bar{B}), \quad M_{8j} = (\bar{A} - \bar{B})g \end{aligned} \tag{20}$$

and

$$\mathbf{w}_j^T[N_j]\bar{\mathbf{w}}_j = \begin{pmatrix} c \\ f \\ R_j \\ R_1 \\ 1 \end{pmatrix}^T \begin{bmatrix} 0 & N_{1j} & N_{2j} & N_{3j} & N_{6j} \\ \bar{N}_{1j} & 0 & N_{4j} & N_{5j} & N_{7j} \\ \bar{N}_{2j} & \bar{N}_{4j} & 0 & 0 & N_{8j} \\ \bar{N}_{3j} & \bar{N}_{5j} & 0 & 0 & -N_{8j} \\ \bar{N}_{6j} & \bar{N}_{7j} & \bar{N}_{8j} & -\bar{N}_{8j} & 0 \end{bmatrix} \begin{pmatrix} \bar{c} \\ \bar{f} \\ \bar{R}_j \\ \bar{R}_1 \\ 1 \end{pmatrix} = 0$$

$$j = 2, \ldots, 8 \tag{21}$$

where

$$\begin{aligned} &N_{1j} = -Q_j\bar{S}_j + Q_1\bar{S}_1, \quad N_{2j} = Q_j\bar{h}, \quad N_{3j} = -Q_1\bar{h}, \\ &N_{4j} = -S_j\bar{h}, \quad N_{5j} = S_1\bar{h}, \quad N_{6j} = (Q_j - Q_1)(\bar{A} - \bar{B}), \\ &N_{7j} = -(S_j - S_1)(\bar{A} - \bar{B}), \quad N_{8j} = (\bar{A} - \bar{B})h \end{aligned} \tag{22}$$

Equations (17), (19), and (21) form 22 synthesis equations of the form

$$\begin{aligned} &\langle c, d, R_j, R_1, 1\rangle\langle \bar{c}, \bar{d}, \bar{R}_j, \bar{R}_1, 1\rangle, \quad j = 2, \ldots, 8, \\ &\langle c, f, R_j, R_1, 1\rangle\langle \bar{c}, \bar{f}, \bar{R}_j, \bar{R}_1, 1\rangle, \quad j = 2, \ldots, 8, \\ &\langle R_j, 1\rangle\langle \bar{R}_j, 1\rangle, \quad j = 1, \ldots, 8 \end{aligned} \tag{23}$$

The bilinear structure of the above equations allows us to place unknowns into the two groups

$$\begin{aligned} &\langle c, d, f, R_1, R_2, R_3, R_4, R_5, R_6, R_7, R_8\rangle, \\ &\langle \bar{c}, \bar{d}, \bar{f}, \bar{R}_1, \bar{R}_2, \bar{R}_3, \bar{R}_4, \bar{R}_5, \bar{R}_6, \bar{R}_7, \bar{R}_8\rangle \end{aligned} \tag{24}$$

The computation of solutions is described in Sec. 5.

4.3 Stephenson III Synthesis Equations. The task of the Stephenson III function generator (Fig. 1(*c*)) is to coordinate links *AD* and *BF* according to the eight pairs of angles (ϕ_j, ψ_j), $j = 1, \ldots, 8$. Note that the input–output function between links *AD* and *CG* is not of interest because they both belong to the same four-bar loop. As well, when *BF* is the output link, the synthesis problem remains the same whether *AD* or *CG* is the input link.

Rotations by the angles ϕ_j, ρ_j, and ψ_j are implemented by the complex vector operators Q_j, R_j, and S_j, respectively. These operators and their conjugates are defined in Eq. (4). The complex pairs $(Q_j, \bar{Q}_j)$ and $(S_j, \bar{S}_j)$ are known from the task specification and $(R_j, \bar{R}_j)$ remain to be solved by the synthesis procedure.

Links *CG* and *FH* are expressed via the loop equations to yield

$$\begin{aligned} &\mathcal{L}_1: \quad G - C = A + Q_j d + R_j g - C, \\ &\mathcal{L}_2: \quad H - F = A + Q_j d + R_j h - B - S_j f, \\ &\qquad j = 1, \ldots, 8 \end{aligned} \tag{25}$$

These links are constrained to be the constant lengths $m = |G - C|$ and $n = |H - F|$. The squares of these lengths are expressed by multiplying $\mathcal{L}_1$ and $\mathcal{L}_2$ by their conjugates to attain

$$\begin{aligned} &\mathcal{C}_1: \ m^2 = (A + Q_j d + R_j g - C)(\bar{A} + \bar{Q}_j\bar{d} + \bar{R}_j g - \bar{C}), \\ &\mathcal{C}_2: \ n^2 = (A + Q_j d + R_j h - B - S_j f)(\bar{A} + \bar{Q}_j\bar{d} + \bar{R}_j\bar{h} - \bar{B} - \bar{S}_j\bar{f}), \\ &\qquad j = 1, \ldots, 8 \end{aligned} \tag{26}$$

By including the eight normalization conditions

$$R_j\bar{R}_j = 1, \quad j = 1, \ldots, 8 \tag{27}$$

we obtain 24 synthesis equations in the 24 unknowns $(R_j, \bar{R}_j)$ and $(C, \bar{C}, d, \bar{d}, f, \bar{f}, m, n)$. Fixed pivots *A* and *B*, and the dimensions *g* and $(h, \bar{h})$ of link *CGH* are specified. Unknowns *m* and *n* are eliminated by subtracting the first equations of $\mathcal{C}_1$ and $\mathcal{C}_2$ from the rest of the equations in each set, respectively. Next, the unknowns are placed in seven sets of vectors

$$\begin{aligned} &\mathbf{v}_j = (d, C, R_j, R_1, 1), \quad j = 2, \ldots, 8, \\ &\mathbf{w}_j = (d, f, R_j, R_1, 1), \quad j = 2, \ldots, 8 \end{aligned} \tag{28}$$

Then, the synthesis equations can be written in the form

$$\mathbf{v}_j^T[M_j]\bar{\mathbf{v}}_j = \begin{pmatrix} d \\ C \\ R_j \\ R_1 \\ 1 \end{pmatrix}^T \begin{bmatrix} 0 & M_{1j} & M_{2j} & M_{3j} & M_{6j} \\ \bar{M}_{1j} & 0 & M_{4j} & M_{5j} & M_{7j} \\ \bar{M}_{2j} & \bar{M}_{4j} & 0 & 0 & M_{8j} \\ \bar{M}_{3j} & \bar{M}_{5j} & 0 & 0 & -M_{8j} \\ \bar{M}_{6j} & \bar{M}_{7j} & \bar{M}_{8j} & -\bar{M}_{8j} & 0 \end{bmatrix} \begin{pmatrix} \bar{d} \\ \bar{C} \\ \bar{R}_j \\ \bar{R}_1 \\ 1 \end{pmatrix} = 0$$

$$j = 2, \ldots, 8 \tag{29}$$

where

$$\begin{aligned} &M_{1j} = -Q_j + Q_1, \quad M_{2j} = Q_j g, \quad M_{3j} = -Q_1 g, \\ &M_{4j} = -g, \quad M_{5j} = g, \quad M_{6j} = (Q_j - Q_1)\bar{A}, \\ &M_{7j} = 0, \quad M_{8j} = \bar{A}g \end{aligned} \tag{30}$$

and

$$\mathbf{w}_j^T[N_j]\bar{\mathbf{w}}_j = \begin{pmatrix} d \\ f \\ R_j \\ R_1 \\ 1 \end{pmatrix}^T \begin{bmatrix} 0 & N_{1j} & N_{2j} & N_{3j} & N_{6j} \\ \bar{N}_{1j} & 0 & N_{4j} & N_{5j} & N_{7j} \\ \bar{N}_{2j} & \bar{N}_{4j} & 0 & 0 & N_{8j} \\ \bar{N}_{3j} & \bar{N}_{5j} & 0 & 0 & -N_{8j} \\ \bar{N}_{6j} & \bar{N}_{7j} & \bar{N}_{8j} & -\bar{N}_{8j} & 0 \end{bmatrix} \begin{pmatrix} \bar{d} \\ \bar{f} \\ \bar{R}_j \\ \bar{R}_1 \\ 1 \end{pmatrix} = 0$$

$$j = 2, \ldots, 8 \tag{31}$$

where

$$\begin{aligned} &N_{1j} = -Q_j\bar{S}_j + Q_1\bar{S}_1, \quad N_{2j} = Q_j\bar{h}, \quad N_{3j} = -Q_1\bar{h}, \\ &N_{4j} = -S_j\bar{h}, \quad N_{5j} = S_1\bar{h}, \quad N_{6j} = (Q_j - Q_1)(\bar{A} - \bar{B}), \\ &N_{7j} = -(S_j - S_1)(\bar{A} - \bar{B}), \quad N_{8j} = (\bar{A} - \bar{B})h \end{aligned} \tag{32}$$

Equations (27), (29), and (31) form 22 synthesis equations of the form

$$\begin{aligned} &\langle d, C, R_j, R_1, 1\rangle\langle \bar{d}, \bar{C}, \bar{R}_j, \bar{R}_1, 1\rangle, \quad j = 2, \ldots, 8, \\ &\langle d, f, R_j, R_1, 1\rangle\langle \bar{d}, \bar{f}, \bar{R}_j, \bar{R}_1, 1\rangle, \quad j = 2, \ldots, 8, \\ &\langle R_j, 1\rangle\langle \bar{R}_j, 1\rangle, \quad j = 1, \ldots, 8 \end{aligned} \tag{33}$$

The bilinear structure of the above equations allows us to place unknowns into two groups

$$\begin{aligned} &\langle C, d, f, R_1, R_2, R_3, R_4, R_5, R_6, R_7, R_8\rangle, \\ &\langle \bar{C}, \bar{d}, \bar{f}, \bar{R}_1, \bar{R}_2, \bar{R}_3, \bar{R}_4, \bar{R}_5, \bar{R}_6, \bar{R}_7, \bar{R}_8\rangle \end{aligned} \tag{34}$$

The computation of solutions is described in Sec. 5.

5 Solution of the Synthesis Equations

The synthesis equations for Watt II, Stephenson II and III function generators each yields a set of 22 equations in 22 unknowns of the form

$$\begin{aligned} &\mathbf{v}_j^T[M_j]\bar{\mathbf{v}}_j = 0, \quad j = 2,\ldots,8, \\ &\mathbf{w}_j^T[N_j]\bar{\mathbf{w}}_j = 0, \quad j = 2,\ldots,8, \\ &R_j\bar{R}_j - 1 = 0, \quad j = 1,\ldots,8 \end{aligned} \tag{35}$$

The Bezout degree for a system of this form is $2^{22} = 4{,}194{,}304$. However, because the equations are bilinear, the general linear bound for this system is $\binom{22}{11} = 705{,}432$ [14,17–19]. The synthesis equations are solved for the dimensions of the function generator by using the numerical homotopy software, BERTINI. Numerical homotopy provides a standardized way to solve these equations [14,20].

Numerical homotopy solves a polynomial system $P(\mathbf{z}) = 0$ by starting with the similar polynomial system $Q(\mathbf{z}) = 0$ with a known set of solutions. The system $Q(\mathbf{z})$ is deformed into $P(\mathbf{z})$ so the solutions of $Q(\mathbf{z}) = 0$ move to become the solutions of $P(\mathbf{z}) = 0$. The tracking of solution paths can be set up as the numerical solution of a set of ordinary differential equations where the solutions of $Q(\mathbf{z}) = 0$ are the initial conditions [18].

Once a general solution is found for the synthesis equations, parameter homotopy continuation is used to increase the efficiency of the computation [14,16]. Parameter continuation is built into the BERTINI software package. The idea behind parameter continuation is to solve Eq. (35) via continuation with the 224 parameters of matrices $[M_j]$ and $[N_j]$, $j = 2,\ldots,8$ specified as random complex numbers. This includes specifying $(M_{qj}, \bar{M}_{qj})$ and $(N_{qj}, \bar{N}_{qj})$ such that they are not complex conjugate pairs. This one-time computation tracks all 705,432 solutions and sorts out the 92,736 nonsingular solutions. The randomly generated parameters are then used in conjunction with these nonsingular solutions to construct straight-line homotopies for Eq. (35), where matrices $[M_j]$ and $[N_j]$ are redefined for synthesis according to Eqs. (10) and (12), Eqs. (20) and (22), or Eqs. (30) and (32). The straight-line homotopies need only to track 92,736 paths. The time required to track all paths of the single generic homotopy took 107 min. The average computational time of the straight-line homotopies reported in this paper was 40 min. All computations were run in parallel on a Mac Pro with 12×2.93 GHz processors.

Note that choosing $M_{qj}, \bar{M}_{qj}, N_{qj}, \bar{N}_{qj}$ as parameters for the general solve that sets up our parameter homotopy makes the structure of Eq. (35) indistinguishable between Watt II, Stephenson II and III cases. However, the general number of synthesis solutions is not necessarily the same between the three cases. Evidence of this is provided in Dhingra et al. [10]. Because of this, our method does not take advantage of further numerical reductions that would be produced by the parameter continuation method if each case were treated individually and the constants internal to coefficients $M_{qj}, \bar{M}_{qj}, N_{qj}, \bar{N}_{qj}$ (Eqs. (9), (11), (19), (21), (29), (31)) were taken as parameters instead.

6 Analysis Equations

The solutions to the forward kinematics equations are used to find all the assembly configurations for a given input value ϕ. We formulate the forward kinematics for each of the three topologies individually. Each assembly configuration is represented by an input value ϕ, and values for angles ρ and ψ, which are found on different loops of the six-bar. As well, for each value of ϕ, there will always be multiple values of ρ and ψ corresponding to different assembly configurations.

6.1 Watt II Analysis Equations. The constraint equations (6) that were used for the synthesis of the Watt II are also used to form its forward kinematics equations

$$\begin{aligned} &C_1(Q,\bar{Q},R,\bar{R}) = (A + Qd - C - Rg)(\bar{A} + \bar{Q}\bar{d} - \bar{C} - \bar{R}\bar{g}) - m^2 = 0, \\ &C_2(Q,\bar{Q},R,\bar{R},S,\bar{S}) = (B + Sf - C - Rh)(\bar{B} + \bar{S}\bar{f} - \bar{C} - \bar{R}\bar{h}) - n^2 = 0 \end{aligned} \tag{36}$$

together with the normalizing conditions

$$\begin{aligned} &N_1(R,\bar{R}) = R\bar{R} - 1 = 0, \\ &N_2(S,\bar{S}) = S\bar{S} - 1 = 0 \end{aligned} \tag{37}$$

Note that the input angle ϕ is represented by $(Q,\bar{Q})$ and the configuration angles ρ and ψ are represented by $(R,\bar{R})$ and $(S,\bar{S})$, respectively. All other parameters are known linkage dimensions.

Equations (36) and (37) form four bilinear equations in the unknowns $(R,\bar{R},S,\bar{S})$. Note that $\{C_1, N_1\}$ form a quadratic subsystem that can be solved independently for two solutions of $(R,\bar{R})$. These solutions can be plugged into $\{C_2, N_2\}$ to form two more systems of two quadratic equations. Each of which has two solutions of $(S,\bar{S})$ for a total of four solutions for a single input pair $(Q,\bar{Q})$.

6.2 Stephenson II Analysis Equations. The constraint equations (16) that were used for the synthesis of the Stephenson II are also used to form its forward kinematics equations

$$\begin{aligned} C_1(Q,\bar{Q},R,\bar{R},S,\bar{S}) &= (A + Qc + Rg - B - Sd) \\ &\times (\bar{A} + \bar{Q}\bar{c} + \bar{R}\bar{g} - \bar{B} - \bar{S}\bar{d}) - m^2 = 0, \\ C_2(Q,\bar{Q},R,\bar{R},S,\bar{S}) &= (A + Qc + Rh - B - Sf) \\ &\times (\bar{A} + \bar{Q}\bar{c} + \bar{R}\bar{h} - \bar{B} - \bar{S}\bar{f}) - n^2 = 0 \end{aligned} \tag{38}$$

along with the normalizing conditions (37) to form four bilinear equations in the unknowns $(R,\bar{R},S,\bar{S})$. McCarthy and Soh [19] use an algebraic elimination procedure to solve equations of this form for the synthesis of a spherical RR chain. His procedure results in a degree six polynomial resultant, the roots of which result in the dimensions of six RR chains. For the case of Eqs. (37) and (38), these roots represent six assembly configurations of a Stephenson II six-bar actuated from link AC.

It is important to note that in this paper we study Stephenson II function generators that move through the accuracy points (ϕ_j, ψ_j), $j = 1,\ldots,8$, where ϕ is the input and ψ is the output. We do not analyze function generators that move through the inverse function, where ψ is the input and ϕ is the output. Although for the latter case the synthesis equations do not change, the analysis of a linkage is dependent upon which parameter is the input. The analysis routine presented in this paper focuses on the elimination of branch defects, and a mechanism's branches are dependent on which link is driven [21].

6.3 Stephenson III Analysis Equations. The forward kinematics equations are formed from the constraint equations (26) to yield

$$\begin{aligned} C_1(Q,\bar{Q},R,\bar{R}) &= (A + Qd + Rg - C) \\ &\times (\bar{A} + \bar{Q}\bar{d} + \bar{R}\bar{g} - \bar{C}) - m^2 = 0, \\ C_2(Q,\bar{Q},R,\bar{R},S,\bar{S}) &= (A + Qd + Rh - B - Sf) \\ &\times (\bar{A} + \bar{Q}\bar{d} + \bar{R}\bar{h} - \bar{B} - \bar{S}\bar{f}) - n^2 = 0 \end{aligned} \tag{39}$$

Combining these equations with the normalizing conditions (37) forms four bilinear equations in the unknowns $(R,\bar{R},S,\bar{S})$. The solution of which follows that of the Watt II forward kinematics equations, resulting in four solutions corresponding to four assembly configurations.

Similar to the Stephenson II case, we have neglected analyzing Stephenson III function generators actuated with ψ as the input and ϕ as the output, despite having synthesis equations identical to those presented in this paper. Also note that the synthesis and analysis procedures are the same whether *AD* or *CG* is the input link and *BF* is the output link.

7 Analysis Procedure

The objective of this analysis is to determine whether the linkage solutions generated by BERTINI are capable of producing a smooth trajectory that moves the input and output links through all required accuracy points. Our notion of a smooth trajectory is defined as a continuous set of configurations that does not pass through a singular point, what others have referred to as a mechanism branch [21,22].

Prior to this analysis, linkage solutions that are not physically realizable or that contain particularly small link lengths are sorted out. The condition for a solution to be physically realizable is that the two variable groups that appear in Eqs. (14), (24), and (34) need to be complex conjugates of each other. The large majority of solutions found are not physically realizable. As well, solutions in which the magnitude of C, d, or f was found to be less than or equal to 0.005 were removed in order to limit solutions with particularly small link lengths.

In this section, we examine all the mechanism branches a linkage is capable of producing and determining whether or not it achieves the desired accuracy points. Mechanism branches are pieced together by solving the forward kinematics equations as presented in Sec. 6 for all assembly configurations for a series of input angles ϕ that represent a full revolution of the input link. Each configuration is sorted into a trajectory according to a sorting algorithm. These trajectories represent mechanism branches. Note that we regard a circuit that possesses no singular points to contain a single mechanism branch.

7.1 Sorting Assembly Configurations. In order to determine the movement of a six-bar linkage, the forward kinematics equations are solved for an array of input angles ϕ_k to obtain $\rho_{k,l}$ and $\psi_{k,l}$, where $l=1,\ldots,6$ identifies the configurations for that input angle. As ϕ_k is incremented, the solutions to these equations do not appear in any order. It is the goal of this section to sort each configuration $(\phi_k, \rho_{k,l}, \psi_{k,l})$ into a smooth trajectory curve.

The input of a mechanism at position k is defined as a vector $\mathbf{x}_k$ and the output as a vector $\mathbf{y}_{k,l}$, such that

$$\mathbf{x}_k = \begin{pmatrix} Q_k \\ \bar{Q}_k \end{pmatrix} \quad \text{and} \quad \mathbf{y}_{k,l} = \begin{pmatrix} R_{k,l} \\ S_{k,l} \\ \bar{R}_{k,l} \\ \bar{S}_{k,l} \end{pmatrix}, \quad l = 1, \ldots, 6 \tag{40}$$

The vector $\mathbf{F}$ is formed such that

$$\mathbf{F}(\mathbf{x}, \mathbf{y}) = \begin{Bmatrix} C_1(\mathbf{x}, \mathbf{y}) \\ C_2(\mathbf{x}, \mathbf{y}) \\ N_1(\mathbf{y}) \\ N_2(\mathbf{y}) \end{Bmatrix} = \begin{Bmatrix} 0 \\ 0 \\ 0 \\ 0 \end{Bmatrix} \tag{41}$$

where the kinematics equations $\{C_1, C_2\}$ are defined in Eqs. (36), (38), or (39) and $\{N_1, N_2\}$ are defined in Eq. (37). The Jacobian of this function is

$$[J_\mathbf{F}] = \left[\frac{\partial \mathbf{F}}{\partial R}, \frac{\partial \mathbf{F}}{\partial S}, \frac{\partial \mathbf{F}}{\partial \bar{R}}, \frac{\partial \mathbf{F}}{\partial \bar{S}}\right] \tag{42}$$

The objective of this algorithm at an input step k is to connect each configuration from set $\mathcal{A}$ to a configuration in set $\mathcal{B}$ where

$$\mathcal{A} = \{(\mathbf{x}_k, \mathbf{y}_{k,l}) \,|\, l = 1, \ldots, 6\} \tag{43}$$

and

$$\mathcal{B} = \{(\mathbf{x}_{k+1}, \mathbf{y}_{k+1,p}) \,|\, p = 1, \ldots, 6\} \tag{44}$$

Note that in general a connecting pair will have $l \neq p$. In order to connect each pair, a Taylor series expansion is used to approximate the kinematics equations at position $k+1$ given by

$$\mathbf{F}(\mathbf{x}_{k+1}, \mathbf{y}_{k+1,l}) \approx \mathbf{F}(\mathbf{x}_{k+1}, \mathbf{y}_{k,l}) + [J_\mathbf{F}]_k(\mathbf{y}_{k+1,l} - \mathbf{y}_{k,l}) \tag{45}$$

In order to estimate the values of $\mathbf{y}_{k+1,l}$ that yield $\mathbf{F}=0$, the approximate values $\tilde{\mathbf{y}}_{k+1,l}$ are computed

$$\tilde{\mathbf{y}}_{k+1,l} = \mathbf{y}_{k,l} - [J_\mathbf{F}]_k^{-1}\mathbf{F}(\mathbf{x}_{k+1}, \mathbf{y}_{k,l}), \quad l = 1, \ldots, 6 \tag{46}$$

These values form the set $\tilde{\mathcal{B}}$ of approximations where

$$\tilde{\mathcal{B}} = \{(\mathbf{x}_{k+1}, \tilde{\mathbf{y}}_{k+1,l}) \,|\, l = 1, \ldots, 6\} \tag{47}$$

If the lth element of $\tilde{\mathcal{B}}$ is sufficiently close to the pth element of $\mathcal{B}$, then the pth element of $\mathcal{B}$ is taken as the neighbor of the lth element of $\mathcal{A}$ on a smooth trajectory. Once each element of $\mathcal{A}$ is connected to a element of $\mathcal{B}$, the algorithm increments to the next step. Cases in which one to one correspondence does not occur are described in Sec. 7.2.

7.2 Identifying Branch Points. The technique described above for sorting the roots of the kinematics equations among assembly configurations can fail at singular and near-singular configurations. That is where

$$\det[J_\mathbf{F}(\mathbf{x}_k, \mathbf{y}_{k,l})] \approx 0 \tag{48}$$

Near-singular configurations can be present even if there is no singularity in the vicinity. Near-singular cases are troublesome because the tracking algorithm can jump from one smooth trajectory to another.

Unlike other methods that explicitly solve for all singular points beforehand [23], our algorithm attempts to sort through the singular points with no prior knowledge to their location. Because singularities mark the input limits of a mechanism, our algorithm sorts configurations whether or not they are entirely physically realizable.

In particular, the tracked curves consist of the elements $(R, S, \bar{R}, \bar{S})$ parameterized by ϕ. Insight to the behavior of curves in this space is given in Fig. 2. This figure plots the real and imaginary components of the output S against the independent input parameter ϕ. Configurations are physically realizable at locations, where $|S| = 1$, that is, where the curves lie on the cylinder. Singular locations were explicitly computed using the method outlined in Myszka et al. [23] for this figure and are marked with purple dots. Note that the curves in Fig. 2 can cross at nonsingular locations because this graph does not include information about R. However, in the higher dimensional configuration space, curves only cross at singular points.

Additionally, note that our analysis and sorting algorithm utilizes a constant step size of angle ϕ. Additional computational benefits may be attained by implementing a variable step size based on proximity to singular locations.

It is near singularities that the algorithm can fail to find a one to one correspondence between sets $\mathcal{A}$ and $\mathcal{B}$ described in Eqs. (43) and (44). Logic is used to address this issue. The set $\mathcal{A}$ contains the last elements of the trajectories arriving at position k, and $\mathcal{B}$

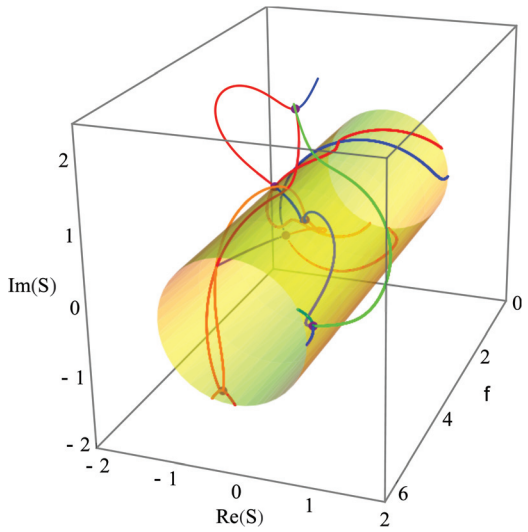

Fig. 2 Example of branch sorting and the presence of singularities

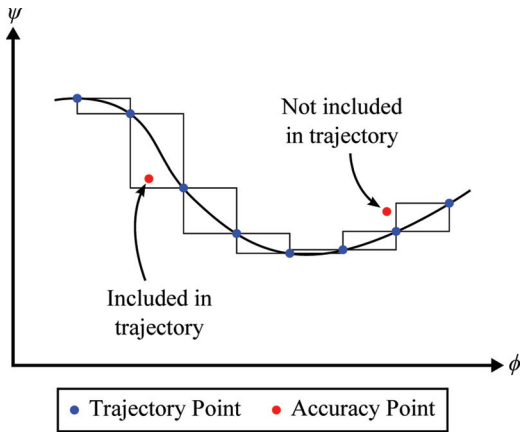

Fig. 3 Criterion used for determining whether a trajectory contains an accuracy point

contains the first elements of the trajectories departing from position $k+1$. At each position we apply the following logic:

(1) If each element of $\mathcal{A}$ connects uniquely to an element of $\mathcal{B}$, the algorithm moves on to the next position.
(2) If an element of $\mathcal{B}$ is not connected to an element of $\mathcal{A}$, that element of $\mathcal{B}$ begins a new trajectory.
(3) If an element of $\mathcal{A}$ connects to multiple elements of $\mathcal{B}$, the trajectory associated with that element of $\mathcal{A}$ is duplicated and each duplicate connects to a matching element of $\mathcal{B}$.
(4) If an element of $\mathcal{A}$ does not connect to an element of $\mathcal{B}$, the trajectory associated with that element of $\mathcal{A}$ is concluded.

Physically realizable sections are separated out upon conclusion of the path tracking algorithm. These sections are then split at points where the sign of the Jacobian determinant changes in order to find cases where the algorithm may jump between trajectories. It is possible for such a jump between trajectories to occur without change in sign of the Jacobian [21]. Our algorithm cannot detect these jumps.

7.3 Determining Useful Designs. Once a six-bar function generator has been designed and mechanism branches have been constructed, it is next determined how many accuracy points lie on a single branch trajectory. Ideally, we prefer to find trajectories that pass through all eight accuracy points. However, we have found that trajectories that pass through seven points and six points can be of practical use as well. Therefore, we enumerate all these mechanisms and leave them for the designer's review.

In order to determine that an accuracy point is on a trajectory, we must decide if the accuracy point is within a specified distance of the list of points that define a trajectory. To do this, it is determined whether an accuracy point is contained in a box defined by two neighboring trajectory points in the ϕ–ψ plane as shown in Fig. 3. Note that six-bar linkages with nonzero error at the accuracy points can satisfy this criterion.

8 Svoboda's Logarithm Linkage

In this section, our design methodology is verified by solving for Watt II six-bar linkages that generate the logarithm function generated by Svoboda's patented design. Figure 4(*a*) shows his "double three-bar" linkage, which is now called a Watt II six-bar linkage. The function that Svoboda mechanized is given by

$$x_2 = \log_{10} x_1, \quad 1 \le x_1 \le 50 \tag{49}$$

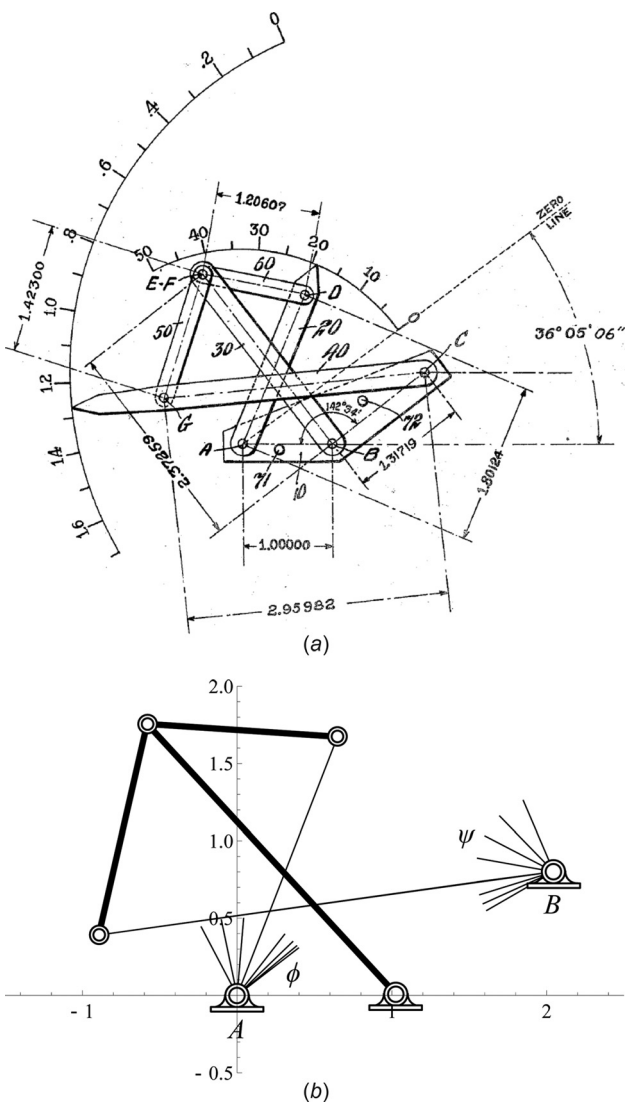

Fig. 4 Comparison of (*a*) Svoboda's logarithm linkage (U.S. Patent 2,340,350, Feb. 1, 1944) and (*b*) the computed Watt II six-bar linkage

Table 1 (a) Accuracy points and (b) specified dimensions attained from Svoboda's linkage design. Points were specified up to 8 decimal digits.

(a) Accuracy points		
j	ϕ_j (deg)	ψ_j (deg)
1	37.71666667	113.16981735
2	39.80000000	134.21966883
3	44.10000000	152.52871342
4	52.20000000	169.93900165
5	68.80000000	187.47879093
6	85.20000000	197.28493451
7	101.80000000	204.41742081
8	117.63333333	210.05171929

(b) Specified dimensions	
A	$0+0i$
B	$2.04592938+0.80063801i$
g	$2.37259+0i$
h	$2.37259+0i$

Table 2 Computation information for Svoboda's logarithm function

Nonsingular solutions	29,395
Physically realizable solutions	953
Eight-point mechanisms	65
Seven-point mechanisms	81
Six-point mechanisms	136
Synthesis computation time	45 min
Analysis computation time	84 min
Analysis timeouts	0
Analysis resolution	0.18009 deg

Table 3 Comparison of Svoboda's design and design found by our algorithm

Dimensions	Original	Computed	Percent difference (%)
C	$1+0i$	$1.02430996+0.01025573i$	2.64
d	$1.80124+0i$	$1.79466456-0.00510634i$	0.46
f	$2.95982+0i$	$2.96851339+0.01689144i$	0.64
m	$1.20607+0i$	$1.23350280+0i$	2.27
n	$1.42300+0i$	$1.40068248+0i$	1.57

He introduced the following scaling so that the variables x_1 and x_2 could be read from the input and output angles, ϕ and ψ, of the linkage

$$\begin{aligned}\phi_{\min} &= 36.08500000 < \phi < \phi_{\max} = 117.63333333\\ \psi_{\min} &= 113.16981735 < \psi < \psi_{\max} = 210.05171929\end{aligned} \tag{50}$$

The result is the function

$$\psi = \frac{\psi_{\max}-\psi_{\min}}{\log_{10} 50}\log_{10}\left(\frac{50(\phi-\phi_{\min})}{\phi_{\max}-\phi_{\min}}\right)+\psi_{\min} \tag{51}$$

Our goal is to find the Watt II six-bar linkages that fit this function at eight accuracy points, Table 1.

BERTINI's parameter homotopy followed 92,736 paths to obtain 29,395 nonsingular solutions. Of these, only 65 linkages were found that passed through all eight accuracy points without a branch defect. A summary of the computational information is provided in Table 2. As noted by McLarnan [9], linkages that may be defective can be useful if they have seven, even six accuracy points on a single branch, which yields an additional 81 and 136 linkage designs, respectively.

A comparison of these linkages with Svoboda's linkage shows that one of the 65 linkages that reach all eight accuracy points has

Table 4 Accuracy points and dimensions specified for the parabolic function generator. For these calculations 300 decimal digits were used.

(a) Accuracy points		
j	ϕ_j (deg)	ψ_j (deg)
1	0	0
2	15	2.5
3	30	10
4	44	21.511111
5	57	36.1
6	69	52.9
7	80	71.111111
8	90	90

(b) Specified dimensions	
A	$0+0i$
B	$1+0i$
g	$0.333333+0i$
h	$0.166667+0.28867514i$

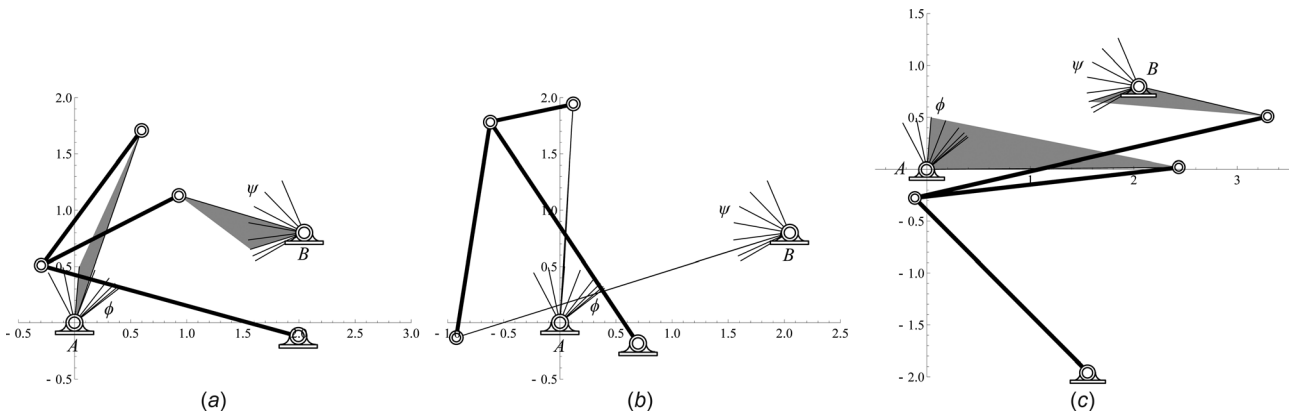

Fig. 5 Three more Watt II six-bar linkages that fit the eight accuracy points of Svoboda's logarithmic function. Each linkage is displayed in the sixth accuracy position.

Table 5 Computation information for synthesis of the parabolic function generators

	Watt II	Stephenson II	Stephenson III
Nonsingular solutions	22,987	64,078	45,763
Realizable solutions	493	141	600
Eight-point mechanisms	86	19	73
Seven-point mechanisms	97	20	113
Six-point mechanisms	95	18	86
Synthesis computation time (min)	37	34	33
Analysis computation time (min)	19	24	30
Analysis timeouts	0	12	0
Analysis resolution (deg)	0.36036	0.36036	0.36036

similar dimensions, Fig. 4. Table 3 shows that the differences between the dimensions that define Svoboda's mechanical computer and our six-bar linkage are less than 3%. Figure 5 presents three other Watt II six-bar linkages that fit the eight accuracy points of Svoboda's logarithm function.

9 Comparison of Six-Bars for Three Functions

In this section, the design of Watt II, Stephenson II and III function generators is carried out for three different task functions. The three functions examined are (i) a parabolic function used by McLarnan [9], (ii) a range ballistic function, and (iii) an elevation ballistic function. The ballistic functions were adapted from an example provided by Svoboda [5].

In each case, the number of defect-free linkages is determined that fit all eight accuracy points, as well as those that have seven and six accuracy points on a single branch. Examples of these designs are provided to illustrate the results.

9.1 Parabolic Function. In this example, designs for Watt II, Stephenson II and III function generators are found for a parabolic function defined by the equation

$$\psi = \frac{1}{90}\phi^2 \tag{52}$$

where ϕ is the input angle and ψ is the output angle measured in degrees. The function is approximated by choosing eight accuracy points. Specified linkage dimensions are shown in Table 4.

BERTINI's parameter homotopy was run for 92,736 paths to obtain 22,987, 64,078 and 45,763 nonsingular solutions, respectively, for the Watt II, Stephenson II and III six-bar function generators, Table 5. For the three cases, there were 86, 19, and 73 useful linkages that achieved the eight accuracy points. Thus, for this function one useful six-bar linkage was found for every 1078, 4881, and 1270 homotopy paths, respectively.

An example design for each mechanism type is shown in Fig. 6. Also shown is a comparison of the specified function and the linkage input–output function with the difference between these functions amplified by 10,000. The largest deviation from the specified function among these three example linkages is found to be 0.025 deg in Fig. 6(*f*).

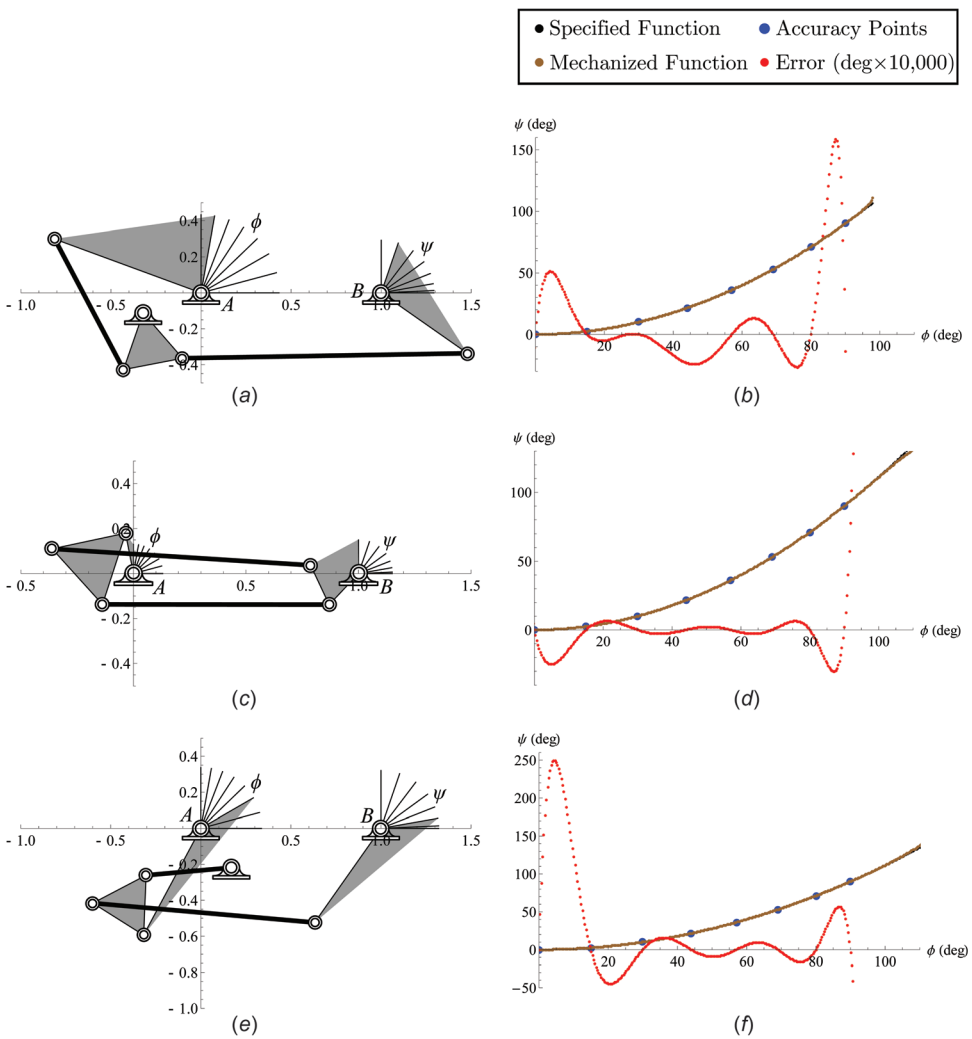

Fig. 6 Design options for the parabolic function for each topology

Table 6 The eight accuracy points and specified dimensions for the range ballistic function. Values were specified up to 300 decimal digits.

(a) Accuracy points		
j	ϕ_j (deg)	ψ_j (deg)
1	0	4.5152437790
2	40	8.9342612197
3	80	13.5874276442
4	115	18.0021905273
5	150	22.9854405071
6	185	29.1127003302
7	210	35.3496863870
8	224	42.5192890583
(b) Specified dimensions		
A		$0-1i$
B		$0+0i$
g		$0.5+0i$
h		$0.25+0.4330127019i$

Table 7 Computation information for synthesis of the range ballistic function generators

	Watt II	Stephenson II	Stephenson III
Nonsingular solutions	23,052	63,753	45,992
Realizable solutions	891	3497	1920
Eight-point mechanisms	1	0	15
Seven-point mechanisms	40	16	77
Six-point mechanisms	80	78	140
Synthesis computation time (min)	35	31	37
Analysis computation time (min)	36	340	126
Analysis timeouts	0	1	3
Analysis resolution (deg)	0.36036	0.36036	0.36036

Examination of the error curve produced by the Watt II design (Fig. 6(*b*)) shows that the error at the fourth accuracy point is not zero, indicating that the displayed trajectory does not pass exactly through this accuracy point. It is actually the case that this linkage has a different branch that does contain the fourth accuracy point. This demonstrates the susceptibility of computational synthesis to numerical error. In this case, two linkage branches are separated by only 0.0025 deg of the accuracy point.

9.2 Range Ballistic Function. Svoboda [5] provides a two degree of freedom linkage that computes the elevation of a gun to hit a target at a given distance and altitude. We separate this into two functions: (i) the range ballistic function that computes the gun elevation angle to reach a given distance at zero altitude and (ii) the elevation ballistic function to reach an altitude at a given range. These calculations assume the muzzle velocity of the artillery round is $v_0 = 500$ m/s and there is no air resistance so that the trajectory is a parabola.

The range ballistic function is designed so that the range scales linearly with the input angle ϕ such that $\phi = 0$ deg is set to 4000 m, and $\phi = 225$ deg is set to 25,484.2 m. The result is the range ballistic function

$$\psi = 45\,\text{deg} - \frac{1}{2}\arccos\left(-\frac{g}{v_0^2}\left(\frac{(25,484.2-4000)\phi}{225}+4000\right)\right) \tag{53}$$

where g is the gravitational constant. This function is approximated by choosing eight accuracy points. Specified linkage dimensions are shown in Table 6.

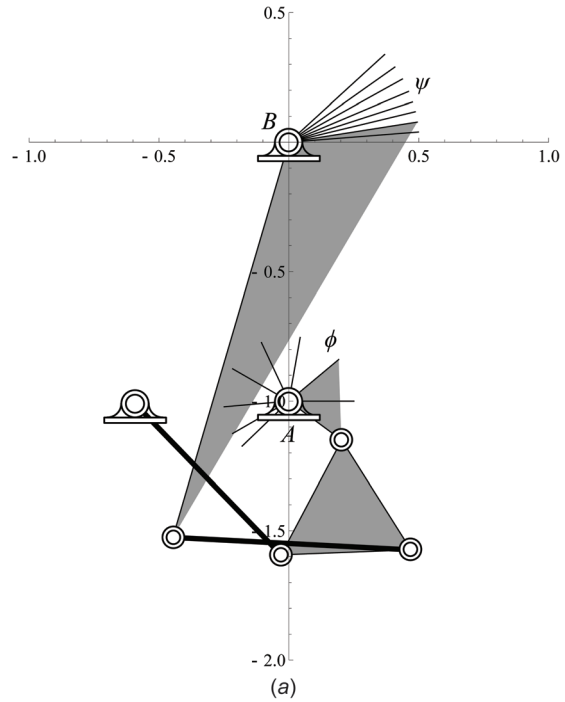

(*a*)

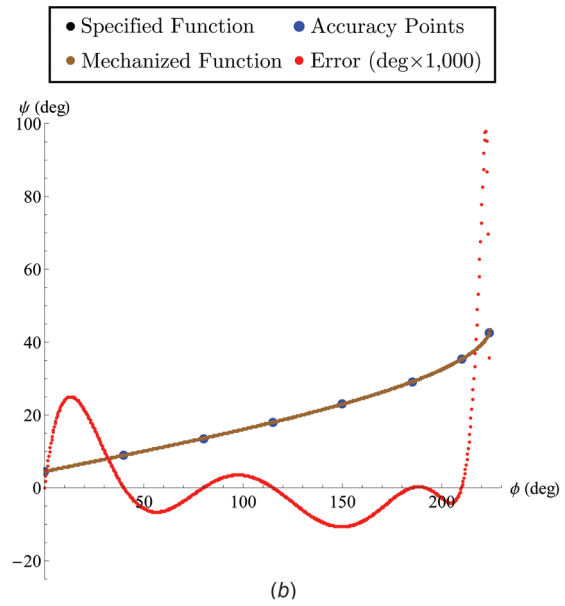

(*b*)

Fig. 7 Design option for the range ballistic function

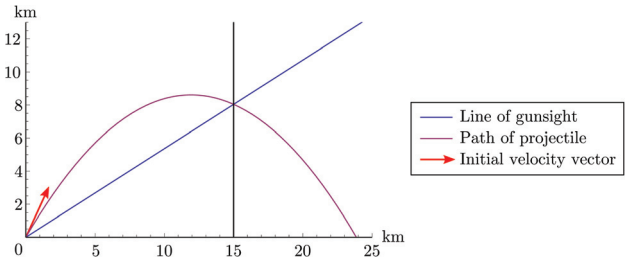

Fig. 8 The line of the gunsight and the parabolic path of the projectile intersect at a horizontal distance of 15 km

Table 8 The eight accuracy points and specified dimensions for the ballistic function. Values were specified up to 300 decimal digits.

(a) Accuracy points

j	ϕ_j (deg)	ψ_j (deg)
1	0	18.0288613860
2	5	23.6695051767
3	10	29.4387864830
4	14	34.1969096229
5	18	39.1602575004
6	22	44.4884326438
7	26	50.6650944462
8	29	58.7006824116

(b) Specified dimensions

A	$0-1i$
B	$0+0i$
g	$0.5+0i$
h	$0.25+0.4330127019i$

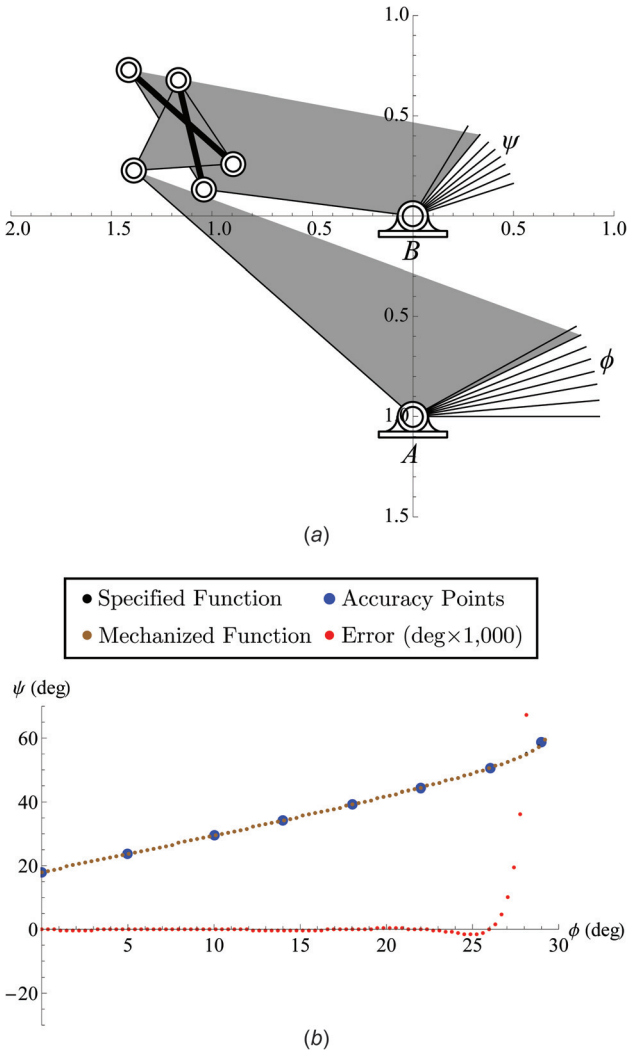

Fig. 9 Design options for the elevation ballistic function

BERTINI's parameter homotopy was run for 92,736 paths and yielded 1, 0, and 15 Watt II, Stephenson II and III six-bar function generators that reach eight accuracy points, Table 7. Thus, useful Watt II and Stephenson II linkages with eight accuracy points for this function were rare. A useful Stephenson III six-bar linkage was found for every 6,182 homotopy paths. Furthermore, examination of each design revealed link lengths of unacceptable dimensions, either too long or too short.

Table 9 Computation information for the elevation ballistic function generators

	Watt II	Stephenson II	Stephenson III
Nonsingular solutions	21,315	60,680	42,691
Realizable solutions	1785	2739	2077
Eight-point mechanisms	83	125	92
Seven-point mechanisms	773	473	691
Six-point mechanisms	415	809	502
Synthesis computation time (min)	45	48	50
Analysis computation time (min)	71	266	114
Analysis timeouts	3	76	18
Analysis resolution (deg)	0.36036	0.36036	0.36036

Figure 7 shows a Stephenson III linkage design that reaches seven accuracy points. Although the designed linkage reaches only seven accuracy points $j=2,\ldots,8$, it does pass close to the remaining accuracy point. A video of this linkage is available at http://www.mechanicaldesign101.com. This is another example of the numerical sensitivity of the computational synthesis process.

9.3 Elevation Ballistic Function. The elevation ballistic function sets the elevation angle of a gun so that a ballistic round reaches a specific altitude at a given range, in this case 15,000 m. The function was constructed so that the input angle ϕ is directed at the target, and the elevation of the gun is the output angle ψ, as shown in Fig. 8. This elevation ballistic function is given by

$$\psi = 45\,\text{deg} + \frac{1}{2}\phi - \frac{1}{2}\arccos\left(-\frac{15,000g}{v_0^2}\cos\phi + \sin\phi\right) \quad (54)$$

This function is approximated with eight accuracy points. Specified dimensions are shown in Table 8. Several useful designs were found for all topologies. A Stephenson II design is shown in Fig. 9.

BERTINI's parameter homotopy was run for 92,736 paths to obtain 83, 125, and 92 useful Watt II, Stephenson II and III six-bar function generators that pass through the eight accuracy points shown in Table 9. This shows that a useful linkage was found in 1 out of 1117, 742, and 1008 homotopy paths, respectively.

10 Summary of Results

This study of the computational synthesis of useful Watt II, Stephenson II, and Stephenson III six-bar linkages shows that a large number of nonsingular solutions must be generated and examined to find useful designs. For the functions presented here, if we consider a useful mechanism to pass through six, seven, or eight accuracy points, then one was found for every 97, 615, and 133 nonsingular solutions on average over the above examples for the Watt II, Stephenson II and III designs, respectively.

The computation time needed to find and analyze each linkage type varied widely as well. It can be seen that the design and analysis of Stephenson II linkages took more time than the other two types of linkages for the above three examples. The Watt II and Stephenson III computation times ranged from 0.9 to 1.1 h, respectively, for the parabolic function, and from 1.9 to 2.7 h for the elevation ballistic function. In contrast, the computation time for the Stephenson II was 1.0, 6.2, and 5.2 h for the three functions. These computations were performed in parallel on a Mac Pro with 12×2.93 GHz processors.

11 Conclusion

This paper examines the synthesis of Watt II, Stephenson II, and Stephenson III six-bar linkages that generate a specified function using eight accuracy points, together with performance verification. This problem was originally formulated in 1963 [9], but the computational resources needed were not available until 1994 [10]. Complete solution of this problem requires not just solution of the synthesis equations but verification that the eight accuracy points lie on one branch. Our results yield a parameter homotopy that tracks 92,736 paths for the eight accuracy point synthesis problem for Watt II, Stephenson II or III six-bar linkages. As well, we evaluate the nonsingular solutions to identify physical linkages, and then evaluate each physical linkage to verify performance.

Three examples were presented: a parabolic function, a range ballistic function, and an elevation ballistic function. For each of the three functions, the Watt II synthesis equations yielded 86, 1, and 83 designs, respectively, that reached all eight accuracy points. Thus, the probability that any particular path of the homotopy will yield a useful linkage is less than one in 1000. Similar results were obtained for the Stephenson II and Stephenson III linkages. The complete design calculation for a particular six-bar linkage type requires approximately 2 h on a Mac Pro with 12×2.93 GHz processors.

Acknowledgment

The authors gratefully acknowledge the support of National Science Foundation award CMMI-1066082. Any opinions, findings, and conclusions or recommendations expressed in this material are those of the authors and do not necessarily reflect the views of the National Science Foundation.

References

[1] Hartenberg, R. S., and Denavit, J., 1964, *Kinematic Synthesis of Linkages*, McGraw-Hill, New York.
[2] Kinzel, E. C., Schmiedeler, J. P., and Pennock, G. R., 2007, "Function Generation With Finitely Separated Precision Points Using Geometric Constraint Programming," ASME J. Mech. Des., **129**(11), pp. 1185–1190.
[3] Plecnik, M., and McCarthy, J. M., 2011, "Five Position Synthesis of a Slider-Crank Function Generator," ASME Paper No. DETC2011-47581.
[4] Kim, B. S., and Yoo, H. H., 2012, "Unified Synthesis of a Planar Four-Bar Mechanism for Function Generation Using a Spring-Connected Arbitrarily Sized Block Model," Mech. Mach. Theory, **49**, pp. 141–156.
[5] Svoboda, A., 1948, *Computing Mechanisms and Linkages*, McGraw-Hill, New York.
[6] Svoboda, A., 1944, "Mechanism for Use in Computing Apparatus," U. S. Patent No. 2,340,350.
[7] Hwang, W. M., and Chen, Y. J., 2010, "Defect-Free Synthesis of Stephenson-II Function Generators," ASME J. Mech. Rob., **2**(4), p. 041012.
[8] Freudenstein, F., 1954, "An Analytical Approach to the Design of Four-Link Mechanisms," Trans. ASME, **76**(3), pp. 483–492.
[9] McLarnan, C. W., 1963, "Synthesis of Six-Link Plane Mechanisms by Numerical Analysis," ASME J. Manuf. Sci. Eng., **85**(1), pp. 5–10.
[10] Dhingra, A. K., Cheng, J. C., and Kohli, D., 1994, "Synthesis of Six-Link, Slider-Crank and Four-Link Mechanisms for Function, Path and Motion Generation Using Homotopy With m-Homogenization," ASME J. Mech. Des., **116**(4), pp. 1122–1131.
[11] Sancibrian, R., 2011, "Improved GRG Method for the Optimal Synthesis of Linkages in Function Generation Problems," Mech. Mach. Theory, **46**(10), pp. 1350–1375.
[12] Wampler, C. W., Sommese, A. J., and Morgan, A. P., 1992, "Complete Solution of the Nine-Point Path Synthesis Problem for Four-Bar Linkages," ASME J. Mech. Des., **114**(1), pp. 153–159.
[13] Wampler, C. W., 1996, "Isotropic Coordinates, Circularity, and Bezout Numbers: Planar Kinematics From a New Perspective," ASME Design Engineering Technical Conferences, Irvine, CA, August 18–22, Paper No. DETC/MECH-1210.
[14] Sommese, A. J., and Wampler, C. W., 2005, *The Numerical Solution of Systems of Polynomials Arising in Engineering and Science*, World Scientific, Singapore.
[15] Erdman, A. G., Sandor, G. N., and Kota, S., 2001, *Mechanism Design: Analysis and Synthesis*, Prentice Hall, Upper Saddle River, NJ.
[16] Morgan, A. P., and Sommese, A. J., 1989, "Coefficient-Parameter Polynomial Continuation," Appl. Math. Comput., **29**(2), pp. 123–160.
[17] Morgan, A. P., and Sommese, A. J., 1987, "A Homotopy for Solving General Polynomial Systems That Respects m-Homogeneous Structures," Appl. Math. Comput., **24**(2), pp. 101–113.
[18] Su, H., McCarthy, J. M., Sosonkina, M., and Watson, L. T., 2006, "Algorithm 857: POLSYS_GLP—A Parallel General Linear Product Homotopy Code for Solving Polynomial Systems of Equations," ACM Trans. Math. Software, **32**(4), pp. 561–579.
[19] McCarthy, J. M., and Soh, G. S., 2010, *Geometric Design of Linkages*, 2nd ed., Springer-Verlag, New York.
[20] Verschelde, J., 1999, "Algorithm 795: PHCpack: A General-Purpose Solver for Polynomial Systems by Homotopy Continuation," ACM Trans. Math. Software, **25**(2), pp. 251–276.
[21] Chase, T. R., and Mirth, J. A., 1993, "Circuits and Branches of Single-Degree-of-Freedom Planar Linkages," ASME J. Mech. Des., **115**(2), pp. 223–230.
[22] Larochelle, P. R., 2000, "Circuit and Branch Rectification of the Spatial 4C Mechanism," ASME Design Engineering Technical Conferences, Baltimore, MD, September 10–13, ASME Paper No. DETC2000/MECH-14053.
[23] Myszka, D. H., Murray, A. P., and Wampler, C. W., 2012, "Mechanism Branches, Turning Curves, and Critical Points," ASME Paper No. DETC2012-70277.